

QFT-Based Robust Simmering Control for Domestic Induction Cookers Using an Infrared Sensor

D. Paesa, C. Franco, S. Llorente, G. Lopez-Nicolas and C. Sagues

Abstract—This paper presents a robust simmering control for induction hobs. This kind of process is almost impossible to carry out in a domestic cooker where the pot temperature is unknown. We exploit an analytical model of the cooking process to design a QFT-based controller. The resultant controller satisfies all user requirements such as a quick heating up, an accurate temperature control and a fast disturbance rejection. Additionally, the proposed temperature control can also minimize the energy consumption and, as a consequence, it can increase the efficiency of the cooking process. Finally, the effectiveness of our proposal has been verified by means of verification test in real induction hobs.

Index Terms—Robust Control, Induction Heating, Home Appliances, Temperature Control.

I. INTRODUCTION

In domestic induction cookers, an inverter topology supplies a high-frequency current to an induction coil, producing an alternating magnetic field. If this field is applied to a ferromagnetic pan, it produces eddy currents and magnetic hysteresis, which heat up the pan. Recently, the domestic induction hobs have become increasingly popular thanks to their specific features such as quick warming, energy saving and high efficiency. Consequently, the research on induction cookers has attracted the attention of theory specialists and practical engineers [1].

The effort to increase the efficiency and the energy saving during a cooking process using an induction hob has been mainly focused on proving to the pot the maximum power in the more efficient way. For instance, designing highly efficient resonant inverter topologies [2], modulation strategies [3], and inductors [4].

However, since the user has no any feedback about how high the temperature is, the user tends to use more power that the cooking process needs. This waste of energy highly decreases the efficiency of the whole cooking process, although the efficiency of the power electronics is very high. Therefore, an improvement in the efficiency during the whole cooking process could be achieved by means of a pan temperature control. Besides, it has more advantages. For instance, the pot temperature control ensures a correct food

cooking minimizing the cooking time and avoiding to reach too high temperatures, which burn the food, or too low temperatures, which cause underdone food. Additionally, it can be used to perform more complicated cooking process such as simmering. During simmering, the food is submerged in water at a temperature from 88°C to 94°C which causes a great effect on the flavour of the food. However, it is almost impossible to carry out in a domestic cooker where the pot temperature is unknown.

The first work related to pot temperature control for induction hobs is [5]. There the authors developed a temperature control for frying pans. Since the pan temperature was not directly measured, it had to be estimated from the measurements of a NTC sensor situated below the ceramic glass. However, that measurement was highly dependent on the cooking load. Therefore, it did not work properly with high-load cooking process such as boiling and deep frying. To overcome this drawback, [6] proposed to use an external infrared sensor rather than a NTC sensor as its shown in Fig. 1. This approach guaranteed an accurate measurement of the pot wall temperature and it was successfully applied to a radiant hob in [7].

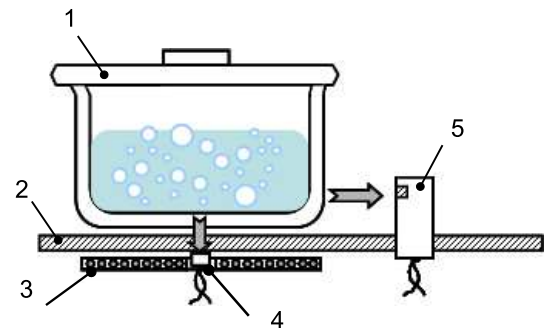


Fig. 1. Main elements of a domestic induction hob. 1: pot. 2: ceramic glass. 3: induction coil. 4: internal NTC sensor. 5: external infrared sensor

In this paper, we present a robust simmering control for domestic induction cookers. It is based on an infrared sensor rather than on a NTC sensor and, as a consequence, it can be applied to high-load cooking process unlike other previous work [5]. Our proposal exploits the potential benefits of using an accurate model of the system [8]. A QFT scheme is designed to guarantee a robust performance. The main contribution of this work compared with [7] is that our control strategy is based on an analytical model of the system rather than on multiple experimental tests. Consequently, the controller tuning process is highly simplified.

This work was supported in part by DGA project PI065/09 and BSH Home Appliances Group.

D. Paesa, C. Franco, G. Lopez-Nicolas and C. Sagues are with Departamento de Informatica e Ingenieria de Sistemas / Instituto de Investigacion en Ingenieria de Aragon, Universidad de Zaragoza, Spain. e-mail: dpaesa@unizar.es, cfranco@unizar.es, gonlopez@unizar.es, csagues@unizar.es

S. Llorente is with the Research and Development Department, Induction Technology, Product Division Cookers, BSH Home Appliances Group, 50016, Zaragoza, Spain. e-mail: sergio.llorente@bshg.com

This paper is organized as follows. In Section II, the state space model of the system is presented. In Section III, a robust control strategy based on the QFT theory is outlined. Some experimental results are shown in Section IV in order to test the robustness of our proposed control scheme. Finally, concluding remarks are outlined in Section V.

II. SYSTEM MODEL

State space model can be used to represent the relation between the power supplied by the induction coil and the temperatures of the system. Generally, state space models are described by the following equation:

$$\begin{aligned}\dot{x}(t) &= A \cdot x(t) + B \cdot u(t) \\ y(t) &= C \cdot x(t)\end{aligned}\quad (1)$$

where $x(t) \in \mathbb{R}^n$ is the state vector, $u(t) \in \mathbb{R}^l$ is the input vector, $y(t) \in \mathbb{R}^m$ is the system output vector and A, B, C are constant $(n \times n), (n \times l), (m \times n)$ matrices.

The model used in this paper is the same that the analytical pot model proposed by [8], thus, how that system is obtained is strongly sketched for brevity. Using an electrical equivalent model that represents the different heat transmissions which appear in our system, and applying the Laplace transform, it is possible to obtain the following state space model:

$$\begin{aligned}\begin{bmatrix} \dot{\theta}_B \\ \dot{\theta}_W \end{bmatrix} &= \begin{bmatrix} a_{11} & a_{12} \\ a_{21} & a_{22} \end{bmatrix} \begin{bmatrix} \theta_B \\ \theta_W \end{bmatrix} \\ &+ \begin{bmatrix} b_{11} & 0 \\ 0 & b_{22} \end{bmatrix} \begin{bmatrix} P \\ Q_E \end{bmatrix} \\ \theta_W &= \begin{bmatrix} 0 & 1 \end{bmatrix} \begin{bmatrix} \theta_B \\ \theta_W \end{bmatrix}\end{aligned}\quad (2)$$

where $\theta_B = T_B - T_0$ is the difference between the pot bottom temperature T_B and the ambient temperature, $\theta_W = T_W - T_0$ is the difference between the pot wall temperature T_B and the ambient temperature, P is the power supplied by the inductor coil which takes into account the efficiency of the electronics and of the inductor and Q_E is the latent heat. Additionally, $a_{11}, a_{12}, a_{21}, a_{22}, b_{11}$ and b_{22} are uncertain parameters that depend on the pot and glass thermal properties as well as on the different thermal losses of the system. Namely, convention losses, radiant losses and conduction losses.

Since the pot which is being used during the simmering process is unknown, these uncertain parameters are initially unknown. However, according to our results obtained during simulation the value of each uncertain parameter is inside a known variation range. Table I summarizes the nominal values of all model parameters and their variations.

Notice that most of cooking process are carry out using a lid, because it highly decreases the thermal losses of the system, and consequently, improves the efficiency. Therefore, we consider that the simmering cooking process is done in a pot with lid which implies that $Q_E = 0$.

TABLE I
NOMINAL MODEL PARAMETERS AND THEIR RANGES

Parameter	Nominal Value	Variations
a_{11}	-0.0197	[-0.0461 -0.0048]
a_{12}	0.0097	[0.00230 0.02291]
a_{21}	0.0018	[0.00030 0.00540]
a_{22}	-0.0010	[-0.0029 -0.0002]
b_{11}	0.0018	[0.00120 0.00290]
b_{22}	0.0001	[0.00010 0.00040]

III. CONTROL SCHEME

Quantitative Feedback Theory (QFT) is a robust control technique developed by Isaac Horowitz [9]. It has been widely used in industrial applications for the last three decades [10], [11], because it takes into account the system parameter uncertainty in the design of the controller.

The first step in QFT design is to translate the system uncertainty to frequency domain. For this purpose, the frequency responses of all possible combinations of system parameters are represented in a Nichols chart. Each point plotted represents a possible plant or sensor for a given frequency. Therefore all these points define a region of the uncertainty of the system at the different working frequencies. These regions are known as templates. In particular, the templates obtained for the uncertain system described in Table I for the working frequencies $\omega = [0.002, 0.005, 0.02, 0.1, 1]$ rad/s are shown in Fig. 2.

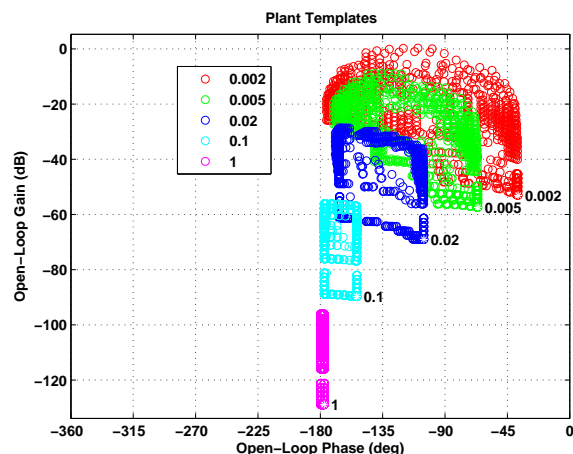


Fig. 2. Plant Templates.

In the next step, control requirements have to be translated into boundaries in a Nichols chart. In QFT, each closed-loop specification, such as robust stability, tracking ability and disturbance rejection, generates a boundary. If the nominal open loop gain avoids the boundaries, it is guaranteed that the closed loop specifications are satisfied for all the plants considered in the template.

For our system, we have selected the following closed-loop performance specifications:

- 1) *Robust Stability*: To ensure robust stability of the closed-loop system, the following constraint on the

peak magnitude of the closed loop frequency response is set:

$$\left| \frac{P(s)G(s)}{1 + P(s)G(s)} \right| \leq \gamma \quad (3)$$

where $P(s)$ is the plant and $G(s)$ is the controller. Moreover, γ is the maximum peak magnitude which corresponds to a minimum gain margin (GM) and phase margin (PM), [12] as follows:

$$GM = 20 \log \left(\frac{\gamma + 1}{\gamma} \right) [dB] \quad (4)$$

$$PM = 2 \sin^{-1} \left(\frac{1}{2\gamma} \right) [deg] \quad (5)$$

in particular, we have chosen $\gamma = 1.5$ which gives $GM = 4.43$ and $PM = 39^\circ$.

- 2) *Reference Tracking*: Due to system uncertainty, we define an acceptable range of variations in the closed loop tracking responses. According to [13], [14], we define an upper $T_{UP}(s)$ and lower $T_{DW}(s)$ bounds for the closed-loop response of our system as follows:

$$|T_{UP}(s)| \leq \left| \frac{P(s)G(s)}{1 + P(s)G(s)} \right| \leq |T_{DW}(s)| \quad (6)$$

Specifically, Fig. 3 shows the upper and lower tracking bounds selected which have the following transfer functions:

$$T_{UP}(s) = \frac{1.02}{(20s + 1)(5s + 1)} \quad (7)$$

$$T_{DW}(s) = \frac{0.98}{(80s + 1)(70s + 1)(1s + 1)(0.1s + 1)} \quad (8)$$

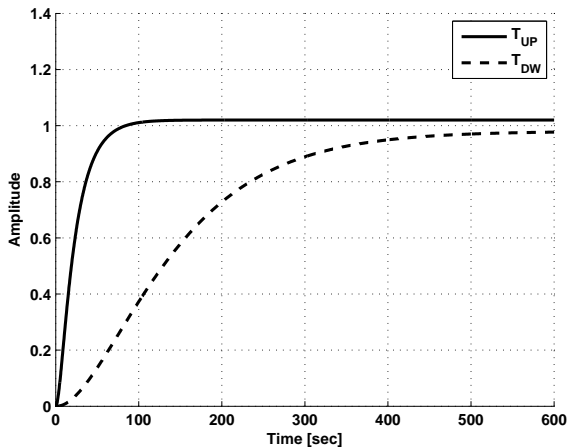


Fig. 3. Step response of the upper and lower tracking bounds.

- 3) *Plant input noise rejection*: According to (2), the power supplied by the inductor is the input of our system which is measured with a Sigma-Delta analog-to-digital converter implemented in the ASIC of the

induction hob [15]. Since this converter has a measurement error about a 5%, we have designed a controller able to reject this kind of disturbances. In particular, we have chosen the following input noise rejection specification:

$$\left| \frac{P(s)}{1 + P(s)G(s)} \right| \leq 0.01 \quad (9)$$

Fig. 4 shows the intersection of these three performance specifications at the design frequencies used during the template generation. To satisfy a performance specifications, the open-loop response has to be above the corresponding boundary as long as it is drawn in solid line, whereas if the boundary is drawn in dashed line the open-loop response has to be below the boundary.

It is easy to see, that the system does not meet the performance specifications since the open-loop frequency response is below the performance specification bounds at each frequency. Therefore, we have to modify the system response adding poles and zeros until the nominal loop lies near its bounds and results in nominal closed-loop stability. This process is known as loop-shaping and generates directly the robust feedback compensator.

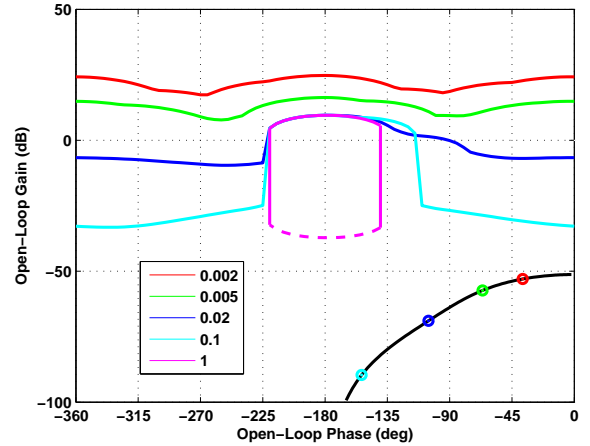


Fig. 4. Open-loop frequency response and performance specification bounds.

Fig. 4 also points out that an appropriate control gain should be introduced to push the open-loop frequency response upwards. Additionally, a dynamic compensator is required in order to change the shape of the open-loop frequency response too. Following this approach, the resulting controller is:

$$G(s) = 9 \frac{\left(\frac{1}{0.0028}s + 1 \right) \left(\frac{1}{0.035}s + 1 \right)}{s \left(\frac{1}{0.9}s + 1 \right)} \quad (10)$$

whose frequency response with the plant is illustrated in Fig. 5. It is clearly seen that the open-loop frequency response meets now all performance requirements, since it is above all bounds at the corresponding frequency. Therefore, we can state that the designed controller ensures robust stability and

an appropriate noise rejection for all of the family of plants defined under the uncertainty shown in Table I.

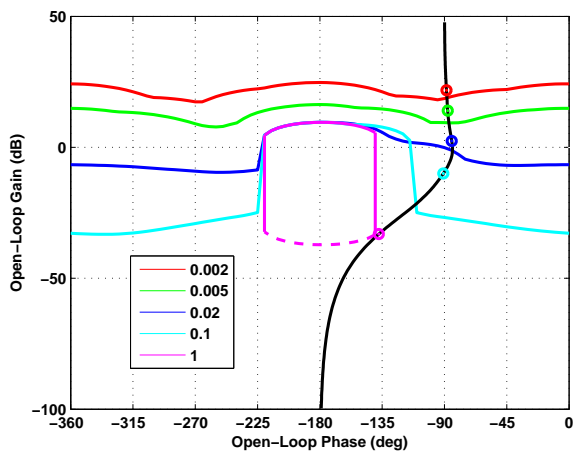


Fig. 5. Open-loop frequency response with the controller.

Nevertheless, the controller is not able to satisfy the tracking specification as it shown in Fig. 6. Therefore, a dynamic pre-filter is required to shape the frequency response to be within the required envelope and attenuate high frequency peaking. Specifically, we have designed the following pre-filter:

$$F(s) = 1 \frac{\left(\frac{1}{0.3}s + 1\right)}{\left(\frac{1}{0.017}s + 1\right) \left(\frac{1}{0.1}s + 1\right)} \quad (11)$$

which allows to meet now the tracking specification as it is shown in Fig. 7.

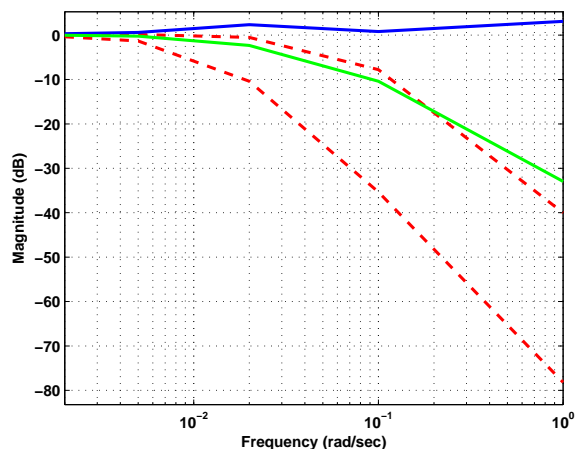


Fig. 6. Closed-loop frequency response with the controller.

So far, we have only ensured that the proposed controller meets the performance requirements at some discrete frequencies. Consequently, an additional checking step at all frequencies inside the working range is needed. For this reason, we show in Figs. 8, 9 and 10 the closed-loop response of the system with the designed controller and pre-filter for

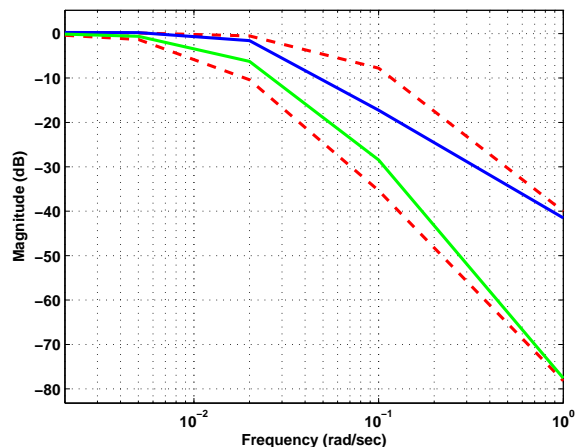


Fig. 7. Closed-loop frequency response with the controller and the pre-filter.

the robust stability, reference tracking and noise rejection specifications respectively.

Concluding, the proposed controller and pre-filter meet the robust stability and noise rejection specifications at all frequencies, since the closed-loop response is below the corresponding boundary in both cases (see Fig. 8 and Fig. 10). Additionally, the proposed controller and pre-filter satisfy also the reference tracking specification, since the maximum and minimum closed-loop response are inside the tracking range defined in (8).

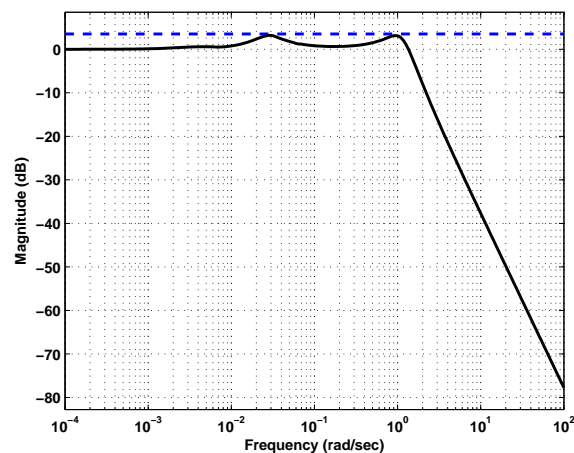


Fig. 8. Closed-loop stability margins.

IV. EXPERIMENTAL RESULTS

Finally, the proposed controller and pre-filter have been implemented in the microcontroller of an real induction hob. Specifically, these algorithms have been programmed in C language. In order to verify that the designed controller and pre-filter work properly, several verification tests on real induction hob were done. Main elements of the induction

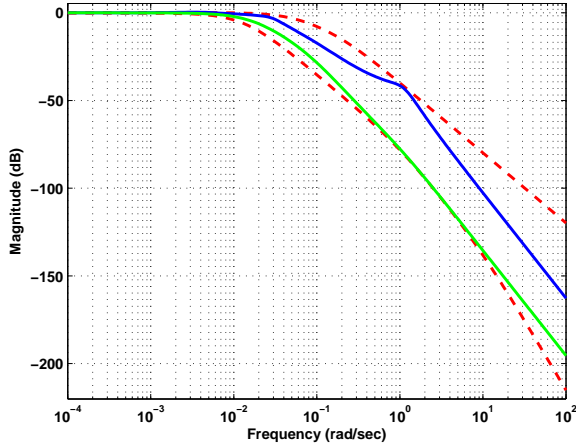


Fig. 9. Closed-loop reference tracking margins.

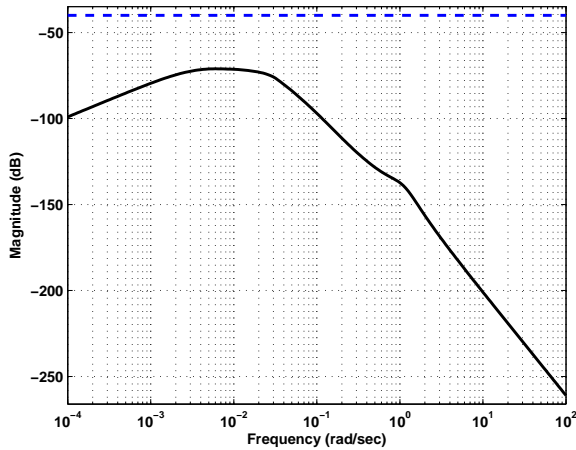


Fig. 10. Closed-loop noise rejection margins.

hob used are shown in Fig. 11 while the real hob used during the verification tests is shown in 12.

Hob takes the energy from the mains voltage; after that, an electromagnetic compatibility filter removes the voltage disturbances, which is subsequently rectified by a full bridge of diodes. Finally, the inverter topology provides to the induction coil the high-frequency current needed to heat up the vessel. The power supplied is controlled modifying the working frequency of the inverter. Consequently, the microcontroller modifies the working frequency of the inverter to provide the desired power. The frequency control algorithm used is described in [16]. The changes of the working frequency are taken in fixed and small steps which ensures stability and convergence of the frequency control algorithm but which causes a transient behavior before the algorithm determines the proper working frequency. Nevertheless, it has no effect in the temperature control, due to the fact that the thermal dynamics are much slower than the inverter topology dynamics.

During the verification tests, the temperature evolution of

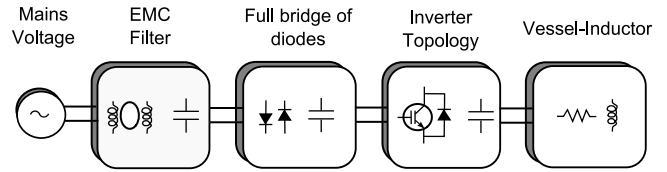


Fig. 11. Arrangement of the induction hob.



Fig. 12. Domestic induction hob used during verification test.

the water during a simmering process is measured. It has to reach a settling temperature between 88°C and 94°C . The software of the microcontroller automatically calculates how much power is needed in order to reach the set point with the minimum rise time but without overshoots. To check the system behavior, we measure the water temperature with an additional thermopile situated inside the water during all the test. Notice that the software does not use the temperature measured by the thermopile. Therefore, this thermopile is not needed in household conditions.

Fig. 13 shows one of the results obtained during the verification tests. We have used a 180mm-diameter induction coil whose maximum power is 1800 watts. The objective is to heat up 1.5 liters of water until the simmering temperature as fast as possible. After that, the controller has to keep the water temperature inside the simmering range. It is easy to see that the proposed controller satisfies both requirements because the water reaches the simmering temperature without overshooting and in just 6 minutes. Additionally, we have tested the robustness of the controller dealing with disturbances. They have been simulated adding 0.5 liters of water more to the pot after the water temperature has reached the simmering temperature. As before, the controller has a proper behavior and brings again the water temperature to the simmering range.

V. CONCLUSION

This paper has presented a water temperature control for domestic induction cookers, which guarantees a proper food cooking and allows to perform more complicate cooking processes such as simmering.

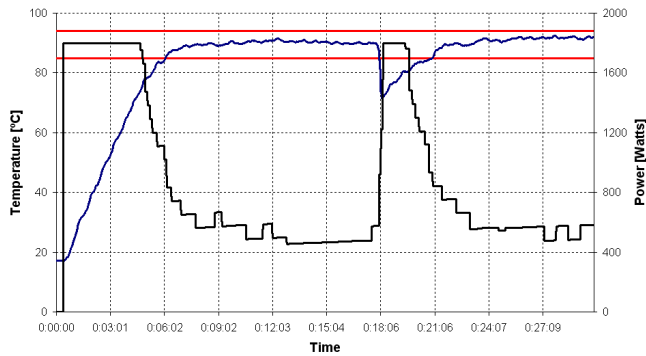


Fig. 13. Verification test. Black line represents the supplied power. Blue line represents the water temperature measured with a thermopile. Area between red lines represents the simmering range.

Since the amount of water and food are initially unknown, a previously developed analytical model has been used to characterize the uncertainty of the process. The controller has been designed according the QFT theory, which is specially well-suited to deal with uncertain systems. According the obtained simulation and experimental results, the proposed QFT-based controller meets all user requirements such as a low settling time, an accurate temperature control within the simmering range and a fast disturbance rejection.

The complete control scheme is robust, safe, and very user friendly. Eventually, it could be applied in consumer induction hobs for automatic cooking.

REFERENCES

- [1] J. Acero, J. M. Burdio, L. A. Barragan, D. Navarro, R. Alonso, J. R. Garcia, F. Monterde, P. Hernandez, S. Llorente, and I. Garde. The domestic induction heating appliance: An overview of recent research. In *Proc. IEEE Applied Power Electronics Conference and Exposition (APEC)*, pages 651–657, 2008.
- [2] J. M. Burdio, F. Monterde, J. R. Garcia, L. A. Barragan, and A. Martinez. A two-output series-resonant inverter for induction-heating cooking appliances. *IEEE Trans. on Power Electronics*, 20(4):815–822, 2005.
- [3] I. Millan, D. Puyal, J. M. Burdio, C. Bernal, and J. Acero. Improved performance of half-bridge series resonant inverter for induction heating with discontinuous mode control. In *Proc. IEEE Applied Power Electronics Conference and Exposition (APEC)*, pages 1293–1298, 2007.
- [4] C. Carretero, J. Acero, R. Alonso, J. M. Burdio, and F. Monterde. Temperature influence on equivalent impedance and efficiency of inductor systems for domestic induction heating appliances. In *Proc. IEEE Applied Power Electronics Conference and Exposition (APEC)*, pages 153–158, 2007.
- [5] D. Paesa, S. Llorente, C. Sagues, and O. Aldana. Adaptive observers applied to pan temperature control of induction hobs. *IEEE Trans. on Industry Applications*, 45(3):1116–1125, 2009.
- [6] U. Has, J. Schieferdecker, and D. Wassilew. Infrared sensor to control temperature of pans on consumer hobs. In *Proc. Int. Congr. OPTO*, pages 247–250, 1998.
- [7] U. Has, J. Schieferdecker, and D. Wassilew. Temperature control for food in pots on cooking hobs. *IEEE Trans. on Industrial Electronics*, 46(5):1030–1034, 1999.
- [8] C. Franco, C. Sagues, D. Paesa, and S. Llorente. Analytical modeling of a saucepan in an induction hob. In *Proc. of the IEEE Mediterranean Control Conference*, (Accepted), 2010.
- [9] Horowitz I.M. A synthesis theory for linear time-varying feedback systems with plant uncertainty. *IEEE Trans. on Automatic Control*, 20(4):454–464, 1975.
- [10] Z. Liu, F. L. L. Luo, and M. H. Rashid. Qft-based robust and precision motion control system for a high speed direct-drive xy table positioning mechanism. In *Conference Record of the IEEE Industry Applications Conference*, volume 1, pages 293–300, 2003.
- [11] C. Lucas, M. M. Shanehchi, P. Asadi, and P. M. Rad. A robust speed controller for switched reluctance motor with nonlinear qft design approach. In *Conference Record of the IEEE Industry Applications Conference*, volume 3, pages 1573–1577, 2000.
- [12] O. Yaniv. *Quantitative Feedback Design of Linear and Nonlinear Control Systems*. Kluwer Academic Publishers, 1999.
- [13] Chait Y. and Yaniv O. Multiple-input/single-output computer-aided control design using the quantitative feedback theory. *Int. Journal of Robust and Nonlinear Control*, 3(1):47–54, 1993.
- [14] A. Banos. Nonlinear quantitative feedback theory. *Int. Journal of Robust and Nonlinear Control*, 17(2):181–202, 2007.
- [15] J. Acero, D. Navarro, L. A. Barragan, I. Garde, and J. M. Burdio. Fpga-based power measuring for induction heating appliances using sigma-delta a/d conversion. *IEEE Trans. on Power Electronics*, 54(4):1843–1852, 2007.
- [16] O. Lucia, J. M. Burdio, I. Millan, J. Acero, and D. Puyal. Load-adaptive control algorithm of half-bridge series resonant inverter for domestic induction heating. *IEEE Trans. on Power Electronics*, 56(8):3106–3116, 2009.